Received: 14 July 2021 | Revised: 7 September 2021 | Accepted: 9 September 2021

DOI: 10.1111/cas.15136

ORIGINAL ARTICLE

Cancer Science WILEY

Curcumin analog GO-Y030 boosts the efficacy of anti-PD-1 cancer immunotherapy

Takashi MaruYama[1,2] | Shuhei Kobayashi[3] | Hiroyuki Shibata[4] | WanJun Chen[1] | Yuji Owada[3]

[1]Mucosal Immunology Section, NIDCR, National Institute of Health, Bethesda, MD, USA

[2]Department of Immunology, Graduate School of Medicine, Akita University, Akita, Japan

[3]Department of Organ Anatomy, Tohoku University Graduate School of Medicine, Miyagi, Japan

[4]Department of Clinical Oncology, Graduate School of Medicine, Akita University, Akita, Japan

Correspondence
Takashi MaruYama, Mucosal Immunology Section, NIDCR, National Institute of Health, Bethesda, MD, USA.
Email: ta-maru@umin.ac.jp

Yuji Owada, Department of Organ Anatomy, Tohoku University Graduate School of Medicine, Miyagi, Japan.
Email: owada@med.tohoku.ac.jp

Funding information
This research was supported in part by the Fund for the Promotion of Joint International Research (Fostering Joint International Research [B]) (18KK0257) to TMY, Grant-in-Aid for Early-Career Scientists (20K19632) to SK, the Intramural Research Program of NIDCR to WC, Grant-in-Aid for Scientific Research (C) (20K11546) to HS, and Joint International Research (B) (20KK0225) and Challenging Exploratory Research (20K21743) to YO

Abstract

Regulatory T cells (Tregs) in the tumor microenvironment regulate tumor immunity. Programmed cell death protein 1 (PD-1) is known to be expressed on Tregs and plays crucial roles in suppressing tumor immunity. However, the immune checkpoint inhibitor, anti-PD-1 antibody, is known to promote the proliferation of the Treg population in tumor-infiltrating lymphocytes, thereby restricting the efficacy of cancer immunotherapy. In this study, we focused on the curcumin analog GO-Y030, an antitumor chemical. GO-Y030 inhibited the immune-suppressive ability of Tregs via metabolic changes in vitro, even in the presence of immune checkpoint inhibitors. Mechanistically, GO-Y030 inhibited the mTOR-S6 axis in Tregs, which plays a pivotal role in their immune-suppressive ability. GO-Y030 also controlled the metabolism in cultured $CD4^+$ T cells in the presence of TGF-β + IL-6; however, it did not prevent Th17 differentiation. Notably, GO-Y030 significantly inhibited IL-10 production from Th17 cells. In the tumor microenvironment, L-lactate produced by tumors is known to support the suppressive ability of Tregs, and GO-Y030 treatment inhibited L-lactate production via metabolic changes. In addition, experiments in the B16-F10 melanoma mouse model revealed that GO-Y030 helped inhibit the anti-PD-1 immune checkpoint and reduce the Treg population in tumor-infiltrating lymphocytes. Thus, GO-Y030 controls the metabolism of both Tregs and tumors and could serve as a booster for anti-immune checkpoint inhibitors.

KEYWORDS
cancer immunotherapy, GO-Y030, metabolism, programmed cell death protein 1, regulatory T cells

Abbreviations: ECAR, extracellular acidification rate; OCR, oxygen consumption rate; PD-1, programmed cell death protein 1; ROS, reactive oxygen species; TGF, transforming growth factor; Tregs, regulatory T cells.

1 | INTRODUCTION

Anti-PD-1 antibody is known to augment antitumor immunity and is therefore called an immune checkpoint inhibitor.[1] However, anti-PD-1 treatment induces the proliferation of Tregs in the tumor microenvironment,[2] leading to the restriction of the antitumor effects. As Treg tumor infiltration and tumor prognosis are negatively correlated,[3] combination therapy with anti-PD-1 to overcome this problem is urgently needed.

Foxp3$^+$ Tregs proliferate and are enriched in the tumor microenvironment, thereby repressing tumor immunity. In the tumor microenvironment, Glut1 expression is higher in Tregs than in effector T cells.[4] TLR8-stimulated inhibition of glycolysis in Tregs significantly reduces their immune-suppressive ability. Moreover, L-lactate promotes the immune-suppressive ability of Tregs in the tumor microenvironment.[5] In anti-PD-1–treated tumor models, glucose concentration in the extracellular milieu of tumors is significantly elevated.[6] Therefore, the control of metabolism in the tumor microenvironment plays a crucial role in cancer immunotherapy.

GO-Y030, a curcumin analog, has been reported to suppress cancer cell growth, and its cancer-suppressive ability is greater than that of curcumin alone in both in vitro and in vivo studies.[7,8] We have previously reported that GO-Y030 represses the immune-suppressive ability of Tregs via blockade of IL-2 signaling.[9] As cellular stress, generated using 2-deoxy glucose, inhibited TGF-β–induced Treg,[10] it can be said that the metabolism of Tregs controls tumor immunity. Here, we found that GO-Y030 induced cellular stress and prevented glycolysis in Tregs. GO-Y030–treated Tregs showed reduced mTOR-S6 axis, which plays a pivotal role in the immune-suppressive ability of Tregs. We also found that GO-Y030 prevented IL-10 production from Th17 cells, which also contributed to repressing tumor immunity.[11] In addition, GO-Y030 treatment significantly inhibited L-lactate production in B16-F10 melanoma cells. In vivo tumor models demonstrated that GO-Y030 treatment reduced the Treg population in the tumor microenvironment and augmented the efficacy of anti-PD-1 cancer immunotherapy. Collectively, our findings suggest that GO-Y030 boosts the efficacy of cancer immunotherapy.

2 | MATERIALS AND METHODS

2.1 | Experimental models

All experiments in this study were performed in accordance with the guidelines approved by the Institutional Animal Care and Use Committee of Akita University, Akita, Japan; the Tohoku University, Japan; and the National Institute of Dental and Craniofacial Research (NIDCR), Bethesda, MD, USA. All methods were performed in accordance with the relevant guidelines and regulations of Akita University, Tohoku University, and NIDCR.

2.2 | Mice

C57BL/6 (CD45.2) mice were purchased from CLEA Japan, Inc and from the Jackson Laboratory. Mice aged 7-12 weeks used in this study were maintained in specific pathogen-free conditions at the animal facilities at Akita University, Tohoku University, and NIDCR.

2.3 | Enzyme-linked immunosorbent assay (ELISA)

ELISA kits for L-lactate assay kit (Cayman Chemicals) were used to quantify the respective cytokines in the culture supernatants according to the manufacturer's protocols. Fluorescence was read in a plate using an excitation wavelength of 530 nm and an emission wavelength of 590 nm by Gen5 (Bio Tek).

2.4 | Flow cytometry

Cells were fixed and permeabilized using the FOXP3 Staining Buffer Kit (eBioscience) and subjected to intranuclear FOXP3 staining according to the manufacturer's instructions. Dead cells were stained with the Zombie Yellow™ Fixable Viability Kit (BioLegend) according to the manufacturer's instructions. The cells were analyzed by flow cytometry using BD LSRFortessa™ (BD Bioscience), BD FACSymphony™ (BD Bioscience), or Canto II (BD Bioscience). Data were analyzed using FlowJo software, Tree-Star version.

2.5 | Antibodies

Pacific Blue–conjugated anti-human CD4 (RPA-T4) and FITC- and Pacific Blue–conjugated anti-mouse CD4 (GK1.5) were purchased from BioLegend. PE-conjugated, APC-conjugated, or Pacific Blue–conjugated anti-mouse Foxp3 antibody (FJK-16S), FITC-conjugated anti-human TCR (IP26), PE-conjugated anti-human CD25 (BC96), PerCP-Cyanine5.5–conjugated anti-human CD4 (OKT4), eFluoro 660–conjugated anti-human Foxp3 (PCH101), PE-conjugated anti-mouse PD-1 (J43), and anti-IFN-γ (R4-6A2) were purchased from eBioscience. APC-conjugated anti-human CD8a (RPA-T8) and PE-conjugated anti-mouse RORγt (B2D) were purchased from Invitrogen. p-S6 (S235/236), ribosomal protein (D57.2.2E), S6 ribosomal protein (54D2), and GAPDH (D16H11) were obtained from Cell Signaling Technology. Anti-mouse PD-1 (29F.1A12) and rat IgG2a isotype control (2A3) were purchased from Bio X cell.

2.6 | T cell cultures

Naïve CD4$^+$ T cells were isolated from mouse spleens using a mouse CD4$^+$CD62L^{hi} T Cell Isolation Kit according to the manufacturer's

instructions (Miltenyi Biotec). Splenic $CD4^+CD25^+$ Tregs were isolated using a mouse $CD4^+CD25^+$ T cell isolation kit according to the manufacturer's instructions (Miltenyi Biotec). Purified cells (approximately 0.5×10^6 cells/mL) were cultured at 37°C in RPMI 1640 containing 10% fetal calf serum, penicillin/streptomycin, and 50 μmol/L 2-mercaptoethanol with 1 μg/mL plate-bound anti-CD3 (eBioscience) and 1 μg/mL soluble anti-CD28 (eBioscience) for 3 days, as indicated in each experiment. For Th17 differentiation, 2 ng/mL TGF-β1 and 50 ng/mL IL-6 were added.

2.7 | Real-time PCR

Total RNA was extracted using the RNeasy Mini Kit (Qiagen), followed by cDNA synthesis using the PrimeScript II 1st Strand cDNA Synthesis Kit (Takara Bio). The resulting cDNA was evaluated by qPCR using an Applied Biosystems 7500 real-time PCR system (Thermo Fisher Scientific) or QuantStudio3 (Thermo Fisher Scientific) instrument and SYBR Premix EX Taq (Takara Bio) or TaqMan Gene Expression Master Mix (Thermo Fisher Scientific). The primer pairs used for qPCR are listed in Table S1.

2.8 | Treg suppression assay

$CD4^+CD25^-$ and $CD4^+CD25^+$ T cells were isolated using the mouse $CD4^+CD25^+$ T Cell Isolation Kit according to the manufacturer's instructions (Miltenyi Biotec). $CD8^+$ T cells were isolated using the mouse $CD8^+$ T Cell Isolation Kit according to the manufacturer's instructions (Miltenyi Biotec). For $CD4^+CD25^+$Treg suppression assay, $CD4^+CD25^+$ T cells were expanded in the presence of 10 ng/mL hIL-2 and 10 μg/mL anti-IFN-γ with 0.25 μmol/L GO-Y030 or 4 mmol/L L-lactate (Cayman Chemical) for 3 days. CellTrace™ Violet Dye (Thermo Fisher Scientific)-labeled naïve $CD8^+$ T cells (0.8×10^5 cells) isolated from CD45.1 mice were cultured in a 96-well plate with Dynabeads™ T-activator CD3/CD28 (Veritask) in the presence or absence of $CD4^+CD25^+$ T cells.

2.9 | Extracellular flux assay

The oxygen consumption rate (OCR) and extracellular acidification rate (ECAR) of B16-F10 melanoma cells were measured using a Seahorse Bioscience XF®96 Extracellular Flux Analyzer (Agilent Technologies). B16-F10 melanoma cells were plated at approximately 25 000 cells/well in Seahorse 96-well plates 24 hours before the assay. B16-F10 melanoma cells were treated with DMSO, curcumin, or GO-Y030 for 2 hours. Then, OCR was measured using the XF Cell Mito Stress Test Kit under basal conditions in response to 1 μmol/L oligomycin and 1 μmol/L of carbonylcyanide p-(trifluoromethoxy) phenylhydrazone (FCCP). Oligomycin injection allowed the calculation of the OCR for ATP production, and FCCP treatment yielded two indices: the maximal OCR capacity and spare respiratory capacity. Finally, OCR was stopped by adding the electron transport chain inhibitors rotenone and antimycin A (0.5 μmol/L each). The Seahorse XF Mito Fuel Flex Test was used to determine the rate of oxidation of each fuel by measuring the OCR. The levels of OCR were normalized to cell number. For Tregs, purified $CD4^+CD25^+$Tregs were isolated from mouse splenocytes using a mouse $CD4^+CD25^+$ T Cell Isolation Kit according to the manufacturer's instructions (Miltenyi Biotec). Then, purified $CD4^+CD25^+$ T cells were expanded in the presence of 10 ng/mL hIL-2 and 10 μg/mL anti-IFN-γ with or without 1 μmol/L curcumin, 0.25 μmol/L GO-Y030, or DMSO for 3 days. Cultured Treg and Th17 cells were plated at approximately 10 000 cells/well and 80 000 cells/well, respectively, onto Seahorse 96-well plates 24 hours before the assay. OCR was measured using the XF Cell Mito Stress Test Kit under basal conditions in response to 1 μmol/L oligomycin and 1 μmol/L FCCP in cultured Tregs or Th17 cells.

2.10 | Tumor model

B16-F10 melanoma cells (approximately 2.5×10^5 cells/100 μL PBS) were subcutaneously injected into the flank of C57/BL6 mice (day 0). Seven days after tumor cell injection, we measured the size of the tumors (length and width), intraperitoneally injected DMSO-PBS, curcumin-PBS (5 mg/kg), or GO-Y030-PBS (5 mg/kg) each day and 200 μg anti-PD-1 (29F.1A12, BioXcell) or control antibody (2A3, BioXcell) every 3 days. Tumor volume (mm^3) was calculated using the following formula: 0.5 × length (mm) × width (mm) × width (mm). Thirteen to sixteen days after tumor cell injection, the tumor specimens were harvested, fixed with ALTFIX, and embedded in OCT compound. Sections (10 μm) were stained using an avidin-biotin complex (Vectastain kit; Vector Laboratories). Nuclei were stained with hematoxylin and eosin.

2.11 | Cell proliferation assay

Naive $CD4^+$ T cells were cultured for 72 hours with 2 ng/mL TGF-β and 50 ng/mL IL-6 (Th17 condition) in the presence or absence of different concentrations of curcumin or GO-Y030. Purified $CD4^+CD25^+$ Tregs from human PBMCs were cultured using FACS sorting Aria II (BD Bioscience) with 10 μg/mL human IL-2 with Dynabeads™ T-activator CD3/CD28 (Veritask) in the presence or absence of GO-Y030 for 72 hours. One tenth volume of the Cell Counting Kit 8 reagent (Apexbio Technology LLC) was added to assess the lactate dehydrogenase activity in live cells. After 4 hours of incubation at 37°C and 5% CO_2, the absorbance was measured at 460 nm using a Spectramax Plus 384 plate reader (Molecular Devices).

2.12 | Statistical analysis

All statistical analyses were performed using GraphPad Prism 5 software (GraphPad Software). Unpaired Student's *t*-test was applied to

two groups. For multiple groups, one-way ANOVA with post hoc Tukey's multiple comparison test was used. Statistical significance was set at $P < .05$. *$P < .05$, **$P < .01$, and ***$P < .001$.

3 | RESULTS

3.1 | Metabolic changes in Tregs by curcumin analog GO-Y030

A previous report demonstrated that limited glucose metabolism induced Th17 cell proliferation and prevented the generation of Tregs.[10] The limitation of glucose metabolism can induce reactive oxygen species (ROS) generation[12] and play crucial roles in Treg/Th17 imbalance. We reported that GO-Y030–treated Tregs showed a low immune-suppressive ability and produced more IL-17A than DMSO-treated Tregs.[9] We also reported that low doses of GO-Y030 (0.25 μmol/L)-treated Tregs did not promote cell death, but reduced the proliferation upon coculture with CD8+ T cells in vitro.[9] To address the mechanisms involved, we examined ROS expression in Tregs and found that ROS expression in GO-Y030–treated Tregs was significantly higher than in curcumin-treated and DMSO-treated Tregs (Figure 1A,B). In addition, OCR under basal conditions of GO-Y030–treated Tregs was significantly lower than that of DMSO- and curcumin-treated Tregs (Figure 1C,D). When we added oligomycin, OCR was significantly reduced in DMSO- and curcumin-treated Tregs, but not in GO-Y030–treated Tregs (Figure 1D,E). We then added a potent mitochondrial oxidative phosphorylation uncoupler FCCP, which revealed that GO-Y030 treatment significantly reduced maximal respiration (Figure 1C,F). We also found that proton leakage was lower in GO-Y030–treated Tregs (Figure 1C,G). mTOR, a member of the PI3-related kinase, is known to control glucose metabolism.[13] Interestingly, in GO-Y030–treated Tregs, the mTOR-ribosomal S6 kinase pathway was not highly active (Figure 1H,I). Thus, GO-Y030 potentially provides antitumor immunity via metabolic changes in Tregs.

3.2 | GO-Y030 controls metabolism processes of human Tregs

GO-Y030 is known to reduce the stability of mouse $CD4^+CD25^+$Tregs.[9] Using the fraction of human $CD4^+CD25^+$Tregs from peripheral blood mononuclear cells (Figure S1A), we found that human $CD4^+CD25^+$Tregs were more resistant to the inhibition of cell proliferation by GO-Y030 compared with mouse $CD4^+CD25^+$Tregs (Figure S1B). We also found

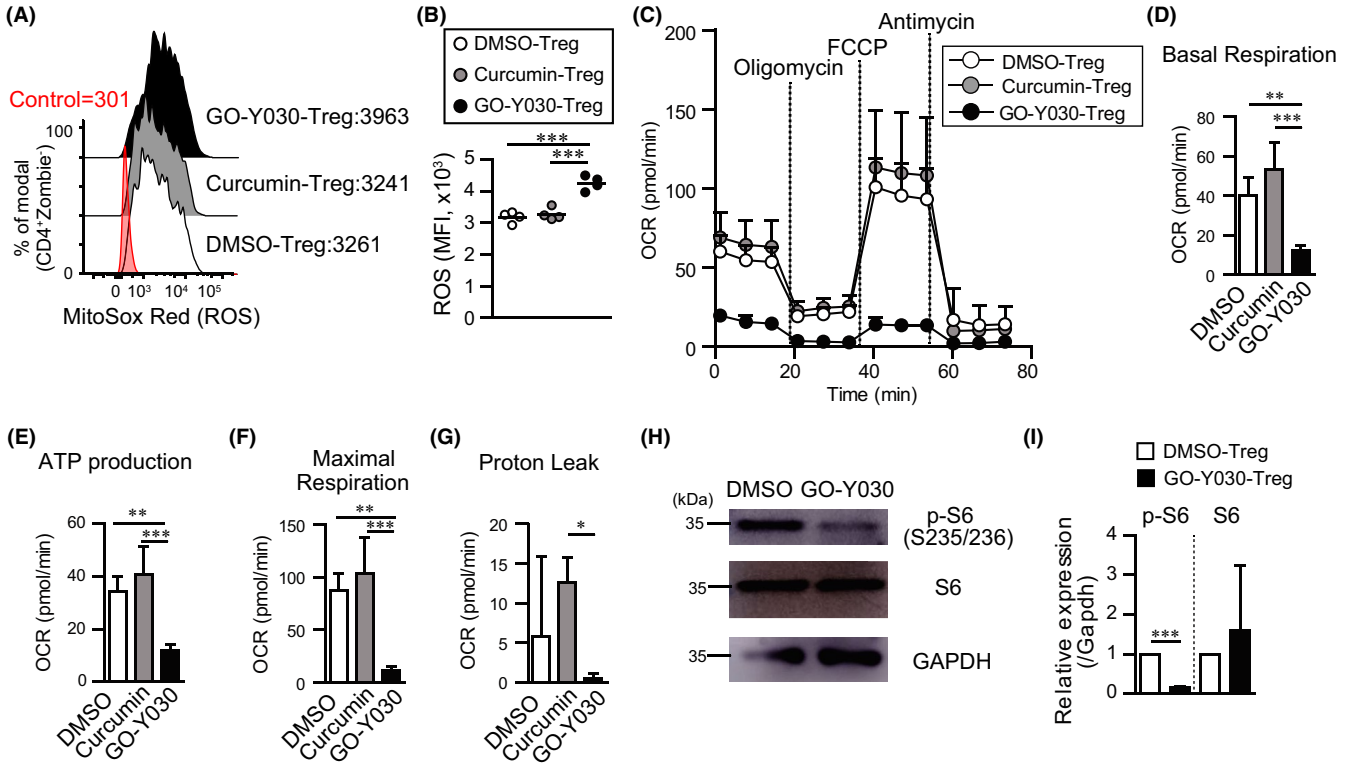

FIGURE 1 GO-Y030 controls metabolism of Tregs. A and B, Reactive oxygen species (ROS) expression in $CD4^+CD25^+$Tregs cultured with 1 μmol/L curcumin, 0.25 μmol/L GO-Y030, or DMSO for 72 h. Data were pooled from four independent experiments. C, Oxygen consumption rate (OCR) was measured under basal conditions or following the addition of oligomycin, carbonylcyanide p-(trifluoromethoxy) phenylhydrazone (FCCP), or rotenone and antimycin A. D-G, Quantification of basal respiration (D), ATP production (E), maximal respiration (F), and proton leak (G) using the rate of OCR. Data were pooled for three independent experiments. One-way ANOVA with post hoc Tukey's multiple comparison test was applied. Data shown are representative of three independent experiments. H and I, Western blotting of cultured Tregs with or without 0.25 μM GO-Y030 for 72 h. Representative pictures at three independent experiments (H). Data were pooled at three independent experiments (n = 4, mean +standard deviation) (I). The relative expression of p-S6 or S6 (/GAPDH) in DMSO Tregs was set as "1"

that GO-Y030 treatment reduced Foxp3 expression in cultured human $CD4^+CD25^+$Tregs in a dose-dependent manner (Figure S1C). Next, we found that GO-Y030 treatment significantly reduced Glut1 (*Slc2a1*) and hexokinase 1 expression (Figure S1D), which play important roles in Treg glycolysis and suppression ability.[14] Thus, GO-Y030 controls the metabolism of human Tregs and impairs the stability of Foxp3 expression.

3.3 | Metabolic changes due to GO-Y030 inhibit IL-10 production from Th17

GO-Y030–treated Tregs showed a Th17 phenotype and reduced the suppression ability without cell death and inhibitory proliferation.[9] We found that 0.25 μmol/L GO-Y030 treatment did not significantly prevent T cell proliferation in the presence of TGF-β+IL-6 compared with DMSO treatment (Figure 2A). In this setting, expression of RORγt, a master regulator of Th17, tended to be highly expressed in GO-Y030 treatment, but there was no significant difference compared with DMSO and curcumin treatment (Figure 2B,C). We also found that *Il17a* expression tended to be highly expressed in GO-Y030 treatment, but there was no difference compared with curcumin and DMSO treatment (Figure 2D). On the other hand, *Il17f* expression was not different between DMSO and GO-Y030 treatment (Figure 2D). Of note, GO-Y030 treatment markedly reduced the expression of *Il10* (Figure 2D), which plays a pivotal role in cancer immunity.[11] We found that GO-Y030 treatment showed significantly lower Glut1 (*Slc2a1*) and hexokinase gene expression than the DMSO control (Figure 2D). In addition, the maximal respiration of GO-Y030 treated Th17 cells was significantly lower than that of DMSO treated Th17 cells

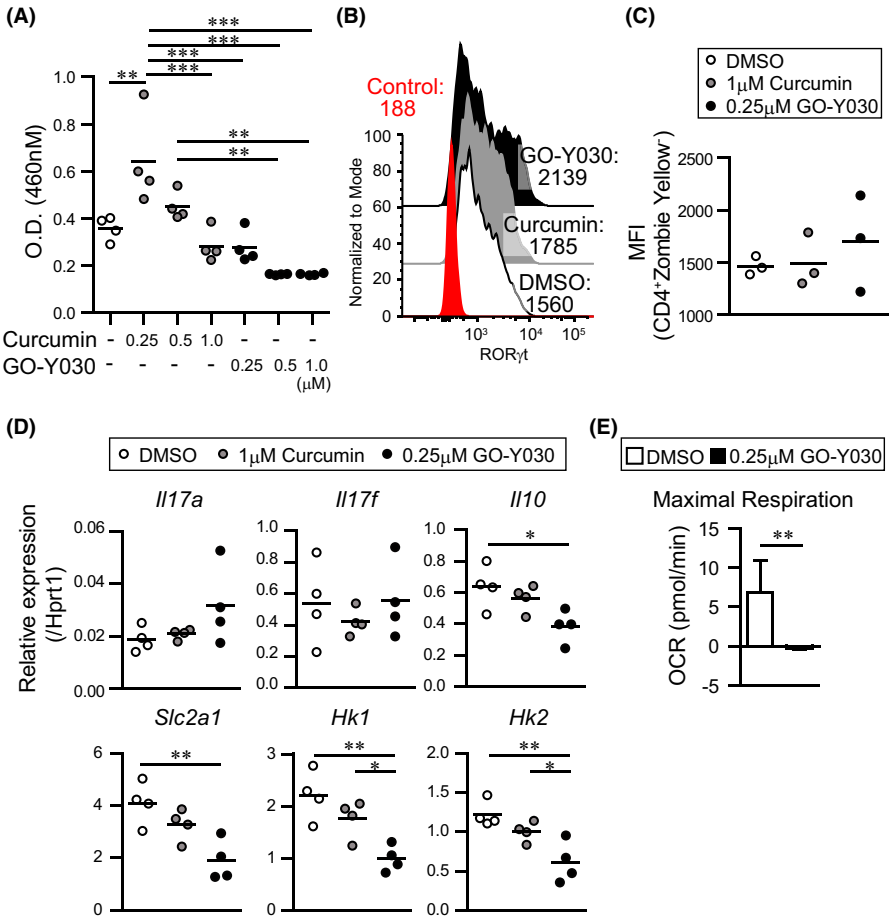

FIGURE 2 GO-Y030 does not prevent Th17 differentiation. A, Relative live cell counts. Naive splenic $CD4^+$ T cells were cultured under Th17 condition (2 ng/mL TGFβ + 50 ng/mL IL-6) and each concentration of curcumin or GO-Y030 as indicated for 72 h, followed by the addition of the cell counting reagent. The circles stand for independent experiments. The horizontal bars represent the mean. B and C, Mean fluorescence intensity (MFI) of RORγt expression in cultured splenic $CD4^+$ T cells under Th17 condition with 1 μmol/L curcumin, 0.25 μmol/L GO-Y030, or DMSO for 72 h. The data show the gated $CD4^+Zombie^-$ population. Red: isotype control, white: DMSO-treatment, gray: curcumin-treatment, black: GO-Y030 treatment. The circles stand for independent experiments. The horizontal bars represent the mean. One-way ANOVA with post hoc Tukey's multiple comparison test was used. D, The real-time quantitative RT-PCR analysis results of DMSO-, 1 μmol/L curcumin-, or 0.25 μmol/L GO-Y030–treated $CD4^+$ T cells for 3 d under Th17 condition. The circles stand for independent experiments. The horizontal bars represent the mean. One-way ANOVA with post hoc Tukey's multiple comparisons test (A, B, C, and D) was used. E, Quantification of maximal respiration using the rate of oxygen consumption rate (OCR). Data were pooled for three independent experiments. Unpaired Student's *t*-test was applied

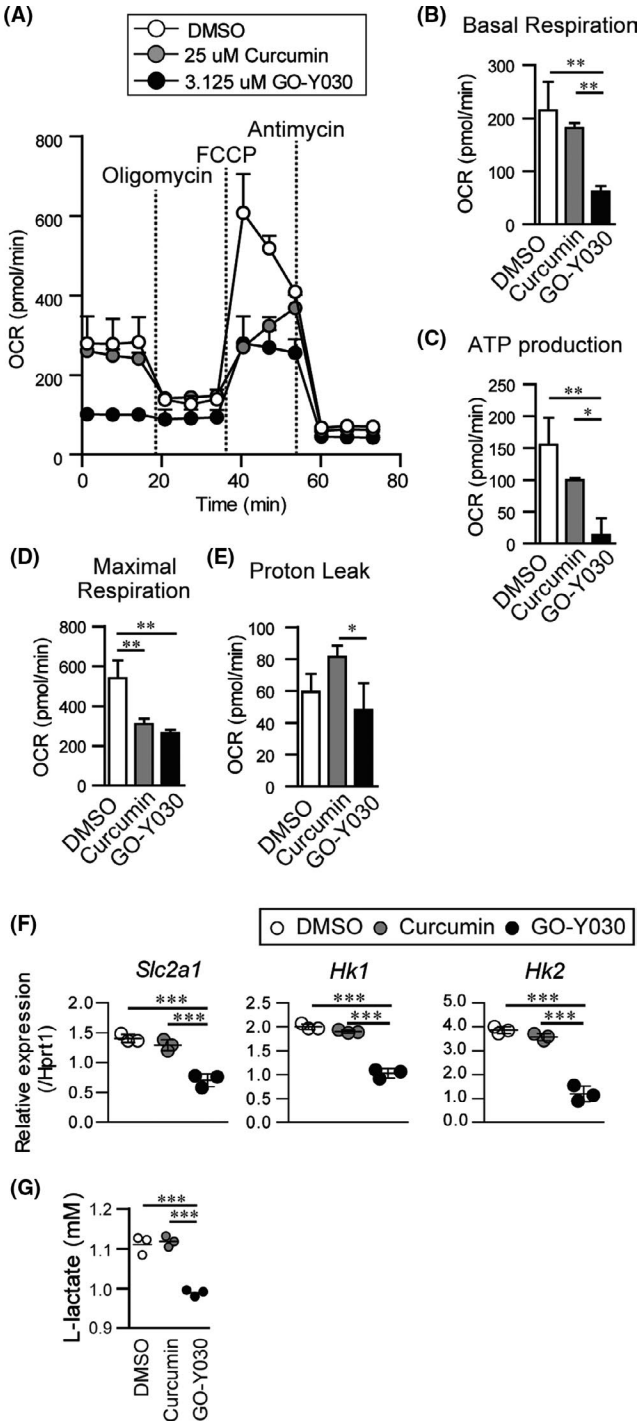

(Figure 2E). Therefore, GO-Y030 controls metabolism in cultured $CD4^+$ T cells and prevents IL-10 production by Th17 cells.

3.4 | GO-Y030 prevents L-lactate production in melanoma cells via metabolic changes

Next, we focused on the metabolism of the GO-Y030–treated melanoma cells. We found that the OCR in the basal condition of GO-Y030–treated B16-F10 melanoma cells was significantly lower

FIGURE 3 GO-Y030 controls the metabolism in B16-F10 melanoma cells. A, Oxygen consumption rate (OCR) was measured under basal conditions or following the addition of oligomycin, carbonylcyanide p-(trifluoromethoxy) phenylhydrazone (FCCP), or rotenone and antimycin A. B-E, Quantification of basal respiration (B), ATP production (C), maximal respiration (D), and proton leak (E) were calculated using the rate of OCR. F, Relative gene expression of DMSO-, 3.125 μmol/L curcumin-, or 3.125 μmol/L GO-Y030–treated B16-F10 melanoma cells for 24 h. G, The level of L-lactate in supernatant from cultured DMSO-, 3.125 μmol/L-curcumin-, or 3.125 μmol/L GO-Y030–treated B16-F10 melanoma cells (16 h). Data were pooled from three independent experiments. One-way ANOVA with post hoc Tukey's multiple comparison test was applied. Data shown are representative of three independent experiments

than that of DMSO- and curcumin-treated cells (Figure 3A,B). When we added oligomycin, an inhibitor of ATP synthase, the OCR in DMSO- and curcumin-treated B16-F10 melanoma cells was significantly reduced, but not in GO-Y030–treated B16-F10 melanoma cells (Figure 3A). This indicated that GO-Y030 treatment inhibited ATP production (Figure 3C). We then added a potent mitochondrial oxidative phosphorylation uncoupler FCCP, which revealed that GO-Y030 treatment significantly reduced maximal respiration (Figure 3A,D). We also found that proton leakage was low in GO-Y030–treated B16-F10 melanoma cells, indicating a reduced ability to convert NADH/FADH to ATP in mitochondria (Figure 3A,E).

Glut1(*Slc2a1*), a membrane protein that facilitates the basal uptake of glucose in the cell, plays an important role in cancer cell proliferation and metastasis.[15] We found that GO-Y030–treated B16-F10 melanoma cells showed significantly lower Glut1 expression than DMSO- or curcumin-treated B16-F10 melanoma cells (Figure 3F). GO-Y030–treated B16-F10 melanoma cells also showed the expression of fewer hexokinase genes (*Hk1* and *Hk2*), which play crucial roles in glycolysis at the initial stage and contribute to ATP synthesis (Figure 3F).

L-lactate from tumor cells is known to maintain the immunosuppressive ability of Tregs in the tumor microenvironment.[5] Our experiments indicated that L-lactate–treated cultured Tregs showed greater suppressive ability than control Tregs (Figure S2A,B). We found that GO-Y030 treatment significantly decreased L-lactate production in B16-F10 melanoma cells compared with DMSO or curcumin treatment (Figure 3G). In the tumor microenvironment, PD-L1 expression in B16-DF10 melanoma cells plays an important role in inhibiting tumor immunity.[16] However, we observed that GO-Y030 had no impact on the expression of PD-L1 in B16-F10 melanoma cells (Figure S3A,B). Thus, GO-Y030 inhibited L-lactate production in B16-F10 melanoma cells via metabolic changes, which repressed the immunosuppressive ability of Tregs in the tumor microenvironment.

3.5 | Curcumin analog boosts the activity of immune checkpoint inhibitor

The expression of the PD-L1 receptor PD-1 on Tregs plays a crucial role in maintaining the immunosuppressive ability of Tregs and

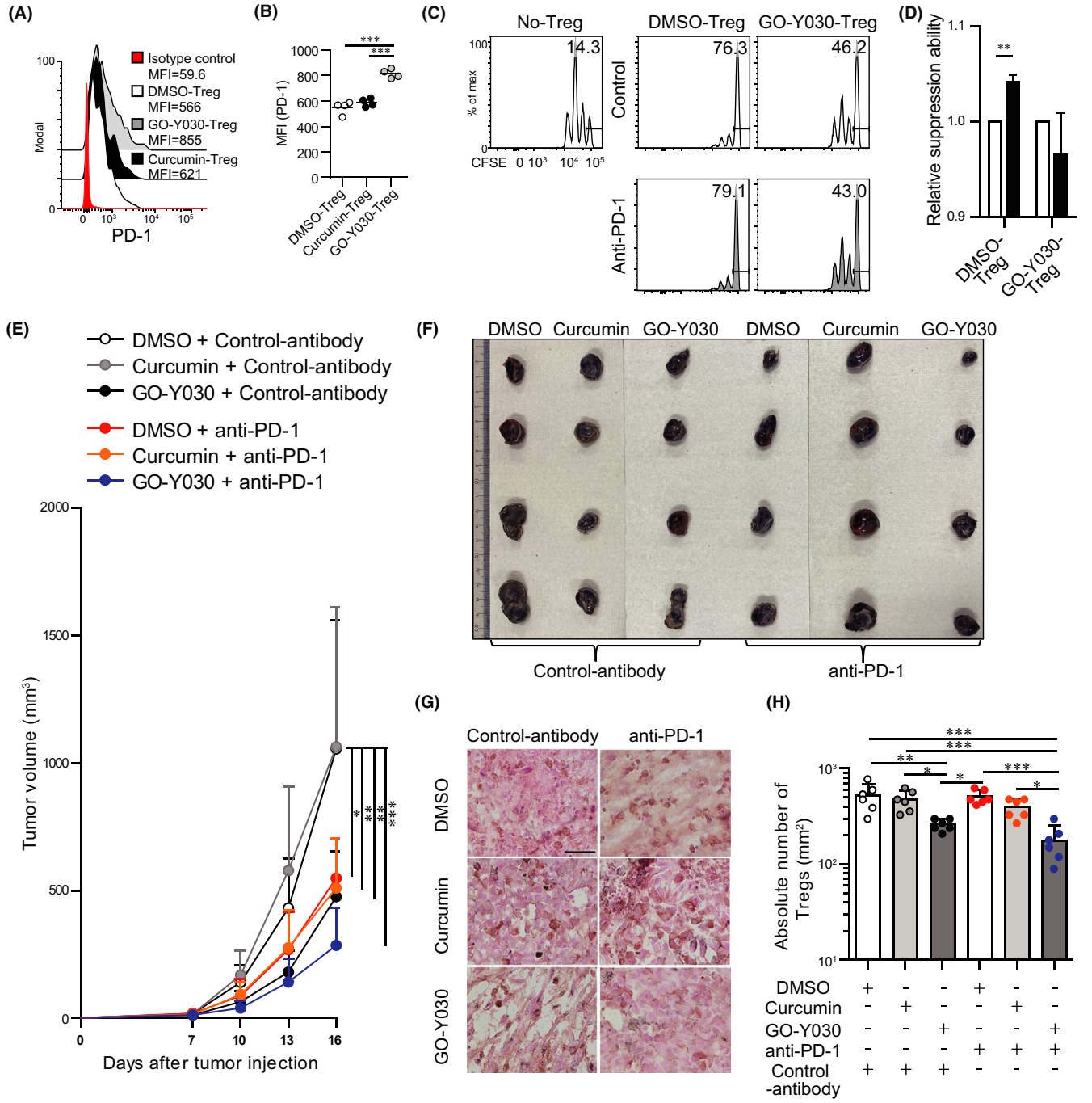

FIGURE 4 GO-Y030 boosts levels of immune checkpoint inhibitors. A and B, Mean fluorescence intensity of PD-1 in cultured Tregs (gated $CD4^+Foxp3^+$Zombie) in the presence of 10 ng/mL IL-2 with or without 1.0 μmol/L curcumin or 0.25 μmol/L GO-Y030 for 72 h. Data are representative of at least three independent experiments. C, Proliferation ratio of CFSE-labeled $CD8^+$ T cells isolated from CD45.1 mice and cultured with or without $CD4^+CD25^+$ Tregs for 48 h ($CD8^+$ T cells : $CD4^+CD25^+$ Tregs = 1:0.5). Tregs were treated with 0.25 μmol/L GO-Y030 or DMSO control for 3 d prior to the coculturing. The $CD8^+CD45.1^+$ gated cell population is as shown. D, Relative suppressive ability of anti-PD-1 antibody. The percentage of suppression ability with control antibody in DMSO or GO-Y030 was set as "1." White: control antibody (10 μg/mL), black: anti-PD-1 (10 μg/mL). The horizontal bars represent the mean. Data were pooled from three independent experiments (n = 3, mean + standard deviation). E, Calculation of tumor volume (mm^3) in each day after 7 d of tumor injection (n = 7-10, mean + standard deviation). Data were pooled from three independent experiments. F, Representative tumors in each group harvested at the end of experiments, as in (E). G, Immunohistochemistry of Foxp3 levels in tumor sites. Representative pictures from three independent experiments (n = 6). Scale bar, 50 μm. The original magnification is 40×. H, Absolute number of $Foxp3^+$Tregs in tumor-infiltrating lymphocytes. One-way ANOVA with post hoc Turkey's multiple comparison test was used (E, G, H). The graph shows mean and standard deviation

tumor progression.[17] We found that GO-Y030 treatment resulted in a higher expression of PD-1 in Tregs than curcumin or DMSO treatment in vitro (Figure 4A,B). Blockade of the PD-1/PD-L1 axis induces the suppressive function of Tregs,[2,18] thereby restricting tumor immunotherapy. We confirmed that blockade of the PD-1/PD-L1 axis in DMSO-treated Tregs tended to increase their immunosuppressive ability (Figure 4C,D). Although GO-Y030–treated Tregs showed reduced immune-suppressive ability,[9] the blockade of the PD-1/PD-L1 axis in GO-Y030–treated Tregs did not show any effects on the immunosuppressive ability of these cells (Figure 4C,D). Thus, GO-Y030 repressed Treg suppression even when the PD-1/PD-L1 axis was blocked in vitro.

Next, we addressed the effect of blocking the PD-1/PD-L1 axis by GO-Y030 treatment on the tumor microenvironment. We found that anti-PD-1 strongly inhibited tumor progression at early time points and cooperated with the GO-Y030 treatment (Figure 4E,F). In the tumor microenvironment, the absolute number of Foxp3$^+$Tregs in the anti-PD-1 antibody plus GO-Y030–treated group was significantly lower than that in the anti-PD-1 antibody with DMSO or anti-PD-1 antibody in the curcumin-treated group (Figure 4G,H). Thus, GO-Y030 has potential as a therapeutic booster against immune checkpoint inhibitory effects in tumors.

4 | DISCUSSION

We have previously reported that GO-Y030–treated CD4$^+$CD25$^+$ Tregs showed low expression of glucose transporter 1 (*Glut1*) and hexokinase (*Hk1* and *Hk2*) genes, which play crucial roles in glycolysis at the initial stage and contribute to ATP synthesis.[19] IL-2 stimulation helps in expanding and stabilizing CD4$^+$CD25$^+$Tregs.[20] mTOR, a member of the PI3-related kinase, can be activated by TCR and IL-2 signaling[21] and plays crucial roles in glucose metabolism.[13] Treg-specific mTOR-deficient mice showed massive inflammation and reduced immune suppression by Tregs.[21] In patients with tumors, FOXP3^{high}CD45RA$^-$CD25^{high} cells can be generated from FOXP3^{low}CD45RA$^-$CD25^{low} cells (called nTregs) in response to antigen stimulation and IL-2, thus contributing to a poor prognosis.[22] Therefore, the metabolism of Tregs in the tumor microenvironment is a good target for regulating tumor immunity.

In this study, we focused on the effects of GO-Y030 on CD4$^+$CD25$^+$Tregs (nTregs) and found that GO-Y030 inhibited glycolysis in vitro, contributing to reduced IL-10 and TGF-β expression and reduced immune suppression by Tregs.[9] We also found that GO-Y030 induced ROS production in Tregs. Because limited glucose metabolism also induces ROS generation[12] and reduces Treg population,[10] ROS induction by limited glycolysis in Tregs using GO-Y030 would reduce the stability and function of Tregs. CD4$^+$CD25$^+$Tregs treated with rapamycin, an mTOR inhibitor, showed low expression of Foxp3 and phosphorylation of Stat5[23]; therefore, mTOR activity in CD4$^+$CD25$^+$Tregs plays a crucial role in their immune-suppressive ability. GO-Y030–treated CD4$^+$CD25$^+$Tregs showed reduced Foxp3 expression in vitro,[9] even in the presence of IL-2 stimulation (data not shown). In this study, GO-Y030 suppressed the mTOR-S6 axis in CD4$^+$CD25$^+$Tregs, thereby reducing their immunosuppressive ability.

A previous report showed that blockade of the PD-1/PD-L1 axis induces the proliferation of PD-1$^+$Tregs in the tumor microenvironment in irradiated mice.[24] Because radiation induces Treg proliferation in the tumor microenvironment,[25] anti-PD-1 treatment may not show sufficient antitumor effects in patients with cancer who received radiation therapy. Our experiments showed that anti-PD-1 treatment did not induce Treg proliferation in the tumor microenvironment of mice (Figure 4H) that did not receive irradiation. Under steady-state conditions, GO-Y030 helped in anti-PD-1–induced tumor immune therapy (Figure 4H). Of note, GO-Y030 does not affect PD-L1 expression in B16-F10 melanoma but prevents L-lactate production, thus potentially preventing Treg proliferation in the tumor microenvironment.[5] Therefore, metabolic changes in Tregs and B16-F10 melanoma cells induced by GO-Y030 treatment can boost immune checkpoint inhibitory effects via multiple steps.

Both TGF-β and IL-6 can be produced by tumors,[26] which contributes to Th17 differentiation. This study demonstrated that GO-Y030 did not prevent Th17 differentiation, but significantly repressed IL-10 production from Th17 cells. We also found that low doses of curcumin (0.25 μmol/L) enhanced the proliferation of cultured CD4$^+$ T cells under Th17 conditions (Figure 2A). However, 0.25 μmol/L curcumin treatment of cultured CD4$^+$ T cells with TGF-β did not show any effect on the proliferation.[9] Low doses of curcumin have been reported to enhance antigen-specific T cells[27] and augment antitumor immunity without inhibiting the suppressive ability of Tregs. Overall, GO-Y030 boosts the immune checkpoint inhibitory effect.

ACKNOWLEDGMENTS

This research was supported in part by the Combined Technical Research Core at NIDCR, NIH. All authors have contributed significantly, and all authors agree with the content of the manuscript.

DISCLOSURE

The authors declare that the research was conducted in the absence of any commercial or financial relationships that could be construed as a potential conflict of interest.

AUTHOR CONTRIBUTIONS

TMY conceived and directed this study, designed and performed most of the experiments, analyzed the data, and wrote the manuscript. SK performed the experiments and analyzed the data. WC and HS provided critical suggestions and materials. YO supervised the experiments and contributed to the manuscript editing.

ORCID

Takashi MaruYama https://orcid.org/0000-0003-0820-3219
Shuhei Kobayashi https://orcid.org/0000-0002-1019-8669
Hiroyuki Shibata https://orcid.org/0000-0003-3581-3506

REFERENCES

1. Okazaki T, Honjo T. PD-1 and PD-1 ligands: from discovery to clinical application. *Int Immunol*. 2007;19:813-824.

2. Kamada T, Togashi Y, Tay C, et al. PD-1(+) regulatory T cells amplified by PD-1 blockade promote hyperprogression of cancer. *Proc Natl Acad Sci USA*. 2019;116:9999-10008.
3. Shang B, Liu Y, Jiang SJ, Liu Y. Prognostic value of tumor-infiltrating FoxP3+ regulatory T cells in cancers: a systematic review and meta-analysis. *Sci Rep*. 2015;5:15179.
4. Xu R, Wu M, Liu S, et al. Glucose metabolism characteristics and TLR8-mediated metabolic control of CD4(+) Treg cells in ovarian cancer cells microenvironment. *Cell Death Dis*. 2021;12:22.
5. Watson MJ, Vignali PDA, Mullett SJ, et al. Metabolic support of tumour-infiltrating regulatory T cells by lactic acid. *Nature*. 2021;591:645-651.
6. Chang C-H, Qiu J, O'Sullivan D, et al. Metabolic competition in the tumor microenvironment is a driver of cancer progression. *Cell*. 2015;162:1229-1241.
7. Sato A, Kudo C, Yamakoshi H, et al. Curcumin analog GO-Y030 is a novel inhibitor of IKKbeta that suppresses NF-kappaB signaling and induces apoptosis. *Cancer Sci*. 2011;102:1045-1051.
8. Shibata H, Yamakoshi H, Sato A, et al. Newly synthesized curcumin analog has improved potential to prevent colorectal carcinogenesis in vivo. *Cancer Sci*. 2009;100:956-960.
9. MaruYama T, Kobayashi S, Nakatsukasa H, et al. The curcumin analog GO-Y030 controls the generation and stability of regulatory T cells. *Front Immunol*. 2021;12:687669.
10. Brucklacher-Waldert V, Ferreira C, Stebegg M, et al. Cellular stress in the context of an inflammatory environment supports TGF-beta-independent T helper-17 differentiation. *Cell Rep*. 2017;19:2357-2370.
11. Martin F, Apetoh L, Ghiringhelli F. Controversies on the role of Th17 in cancer: a TGF-beta-dependent immunosuppressive activity? *Trends Mol Med*. 2012;18:742-749.
12. Kajihara N, Kukidome D, Sada K, et al. Low glucose induces mitochondrial reactive oxygen species via fatty acid oxidation in bovine aortic endothelial cells. *J Diabetes Investig*. 2017;8:750-761.
13. Saxton RA, Sabatini DM. mTOR signaling in growth, metabolism, and disease. *Cell*. 2017;169:361-371.
14. Li L, Liu X, Sanders KL, et al. TLR8-mediated metabolic control of human Treg function: a mechanistic target for cancer immunotherapy. *Cell Metab*. 2019;29(1):103-123.e5.
15. Zambrano A, Molt M, Uribe E, Salas M. Glut 1 in cancer cells and the inhibitory action of resveratrol as a potential therapeutic strategy. *Int J Mol Sci*. 2019;20(13):3374.
16. Hu Z, Yu P, Du G, et al. PCC0208025 (BMS202), a small molecule inhibitor of PD-L1, produces an antitumor effect in B16–F10 melanoma-bearing mice. *PLoS One*. 2020;15:e0228339.
17. DiDomenico J, Lamano JB, Oyon D, et al. The immune checkpoint protein PD-L1 induces and maintains regulatory T cells in glioblastoma. *Oncoimmunology*. 2018;7:e1448329.
18. Dodagatta-Marri E, Meyer DS, Reeves MQ, et al. alpha-PD-1 therapy elevates Treg/Th balance and increases tumor cell pSmad3 that are both targeted by alpha-TGFbeta antibody to promote durable rejection and immunity in squamous cell carcinomas. *J Immunother Cancer*. 2019;7:62.
19. Meng Y, Xu XI, Luan H, et al. The progress and development of GLUT1 inhibitors targeting cancer energy metabolism. *Future Med Chem*. 2019;11:2333-2352.
20. Chinen T, Kannan AK, Levine AG, et al. An essential role for the IL-2 receptor in Treg cell function. *Nat Immunol*. 2016;17:1322-1333.
21. Zeng H, Yang K, Cloer C, Neale G, Vogel P, Chi H. mTORC1 couples immune signals and metabolic programming to establish T(reg)-cell function. *Nature*. 2013;499:485-490.
22. Tanaka A, Sakaguchi S. Regulatory T cells in cancer immunotherapy. *Cell Res*. 2017;27:109-118.
23. Procaccini C, De Rosa V, Galgani M, et al. An oscillatory switch in mTOR kinase activity sets regulatory T cell responsiveness. *Immunity*. 2010;33:929-941.
24. Kumagai S, Togashi Y, Kamada T, et al. The PD-1 expression balance between effector and regulatory T cells predicts the clinical efficacy of PD-1 blockade therapies. *Nat Immunol*. 2020;21:1346-1358.
25. Liu S, Sun X, Luo J, et al. Effects of radiation on T regulatory cells in normal states and cancer: mechanisms and clinical implications. *Am J Cancer Res*. 2015;5:3276-3285.
26. Fisher DT, Appenheimer MM, Evans SS. The two faces of IL-6 in the tumor microenvironment. *Semin Immunol*. 2014;26:38-47.
27. Hayakawa T, Yaguchi T, Kawakami Y. Enhanced anti-tumor effects of the PD-1 blockade combined with a highly absorptive form of curcumin targeting STAT3. *Cancer Sci*. 2020;111:4326-4335.

SUPPORTING INFORMATION

Additional supporting information may be found in the online version of the article at the publisher's website.

How to cite this article: MaruYama T, Kobayashi S, Shibata H, Chen W, Owada Y. Curcumin analog GO-Y030 boosts the efficacy of anti-PD-1 cancer immunotherapy. *Cancer Sci*. 2021;112:4844–4852. https://doi.org/10.1111/cas.15136